Investigations of eddy current vibration damping

Karel RUBER[1]; Sangarapillai KANAPATHIPILLAI[2]; Robert RANDALL[3]

[1,2,3] School of Mechanical and Manufacturing Engineering, The University of NSW (UNSW), Sydney, Australia

ABSTRACT

Eddy currents are generated in electrically conductive materials such as copper in response to a moving magnetic field and they generate forces in the opposite direction of the relative movement of the magnetic field to the conductive material. Those forces have been used for braking applications and are proportional to the relative velocity between the conductive material and the magnetic field, similar to viscous damping forces in vibration attenuation applications.

This paper investigates various geometrical configurations of magnet and copper assemblies with the purpose of quantifying and maximising the eddy current forces. The effects of air gaps, magnetic field strength, orientation and surface area are investigated with Finite Element Analysis (FEA) and validated with measurements.

1. INTRODUCTION

The phenomena of eddy currents was discovered in the 19th century and it has been applied to braking of machinery and vehicle braking for decades.

The principle of the eddy current forces phenomena is that a change in the magnetic field surrounding an electrical conductor induces an electrical potential in the conductor which creates electrical currents. The induced currents create a magnetic field which opposes the changes in the magnetic field that created the currents.

Faraday's law states that an electromagnetic force (emf) is generated in a conductor whenever there is a change in the magnetic field and the emf ε [V] is equal to the rate of change of the magnetic field expressed by the magnetic flux density $\varnothing_B$ [Tesla], experienced by the conductor (1).

$$\varepsilon = -\frac{d\phi_B}{dt} \qquad \textbf{(1)}$$

In the case of a wire conductor, the emf creates a current I[A] which is proportional to the resistance R[Ohms] of the wire. In the case where the conductor is a solid body (or when the skin effect is considerable such as in the case of high frequency excitations) – the induced current density J [A/m^2] is proportional to the conductor's material resistivity ρ [Ohms·m] and to the electric field E [V/m].

$$I = \frac{\varepsilon}{R} \quad and \quad \vec{J} = \frac{\vec{E}}{\rho} \qquad \textbf{(2)}$$

Lentz's law states that the induced currents will create a magnetic field in a direction that will oppose the changes in the magnetic field that induces the currents which is shown by the minus sign in equation 1.

Eddy currents flowing in an electrical conductor create Lorentz forces F_L [N] that oppose the relative movement between the conductor and the magnetic field. In absence of an electrical field

Lorentz forces are equal to the cross product of the current and the magnetic flux density. If the current density is not uniform then the Lorentz forces density F_{Lt} [N/m^3] is calculated from the induced current density J instead of the current. The Lorentz forces can be calculated by integrating the Lorentz forces density.

$$\vec{F}_L = \vec{I} \times \vec{B} \ \ and \ \ \vec{F}_{Lt} = \vec{J} \times \vec{B} \tag{3}$$

Bae at al (2) investigated analytically and experimentally the characteristics of eddy current damping when a permanent magnet was moving inside a copper tube. The steady-state damping force was measured and calculated from the terminal velocity of the magnet during a free fall in the tube. A dynamic-state damping was measured by exciting the magnet with a low frequency (<8 Hz) sinusoidal motion and both measurement results were compared against theoretical results. One of the main finding was that above approximately 4 Hz the measured dynamic-state damping results diverge from the predicted and measured steady state results.

The research presented in this paper investigates the effects of geometrical and physical parameters of the conductive pipe and magnet on the eddy current damping magnitude. The validation of the FEA model is done by comparison of the Impedance of the mass and eddy damper system measured with a broad band excitation between 7 Hz and 200 Hz.

2. Model Configurations and Investigated Effects

An axisymmetric 2D FEA Model of Magnet and Pipe was created and analysed using the Comsol Finite Element Analysis (FEA) multi-physics package and the ACDC module.
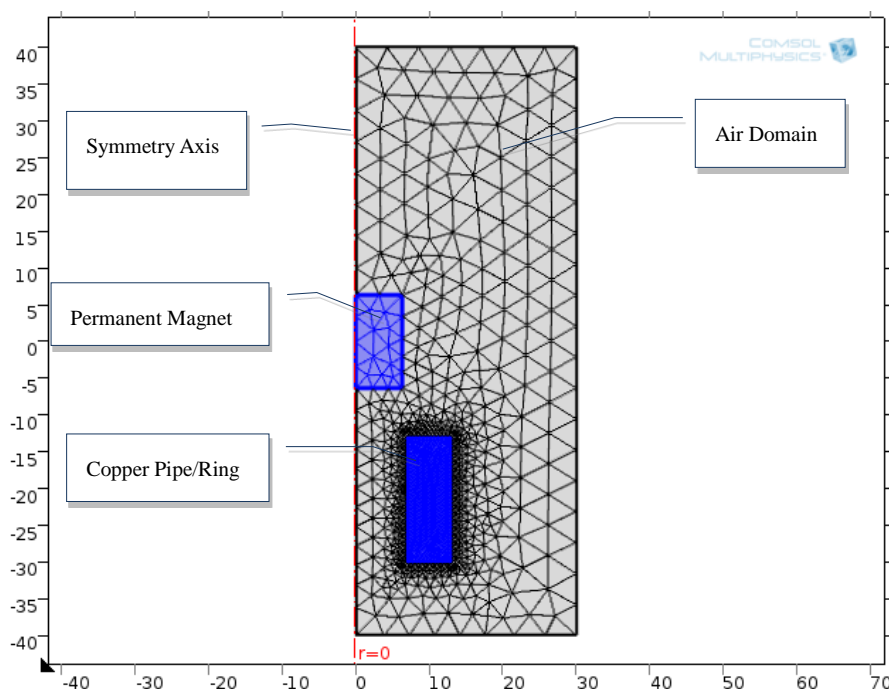

Figure 1 –2D Axisymmetric FEA Model of Magnet and Pipe. The pipe is moving upward at 1 mm steps with a constant velocity.

The effect on the induced eddy currents and Lorentz forces of 5 geometrical and 1 physical parameters were investigated by creating a parametric model in Comsol:

1. Magnet Diameter [mm]

2. Magnet Length [mm]

3. Pipe Thickness [mm]

4. Pipe Length [mm]

5. Air Gap [mm]

6. Velocity [mm/sec]

Each parameter was defined at three levels and only one variable changed in each run, no cross interaction effects were studied at this time.

2.1   FEA validation against Test Results

In order to validate the FEA model and analysis results, test were conducted on two samples of magnets and short copper pipes (rings) using an electro dynamic shaker to generate a random vibration excitation in the range of 7Hz-200Hz. The moving part was the magnet which was attached to a small permanent magnet shaker LDS V201, through an impedance head B&K 8001 which measured simultaneously the forces and acceleration of the magnet while the copper part was held steady.
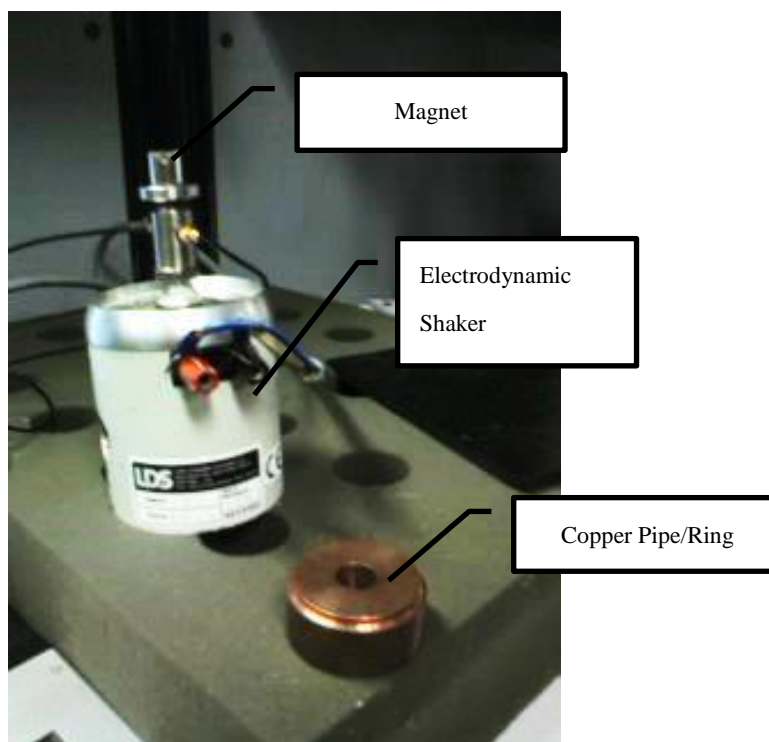

Figure 2–Shaker, magnet and copper pipe (ring)

The acceleration signal was integrated to give velocity and the driving point transfer function (or more correctly called Frequency Response Function) H1 between the Force and Velocity of the magnet was calculated by the B&K Pulse FFT analyser and displayed as an Impedance Magnitude spectrum [N·s/m]. A typical screen capture of Pulse s/w is shown below in Figure 3.

All magnet samples were permanent cylindrical magnets axially magnetised and made of Neodymium (NdFeB) with a rating of N42. The magnetic remanence was between 0.56 T and 1.1 T. In the first test configuration a magnet with diameter and length of 12.7 mm was tested with a short copper pipe (ring): inner diameter (ID) 13 mm, outer diameter (OD) 44 mm and length 15.5 mm. This configuration of magnet and copper ring is referred to as Config 1.
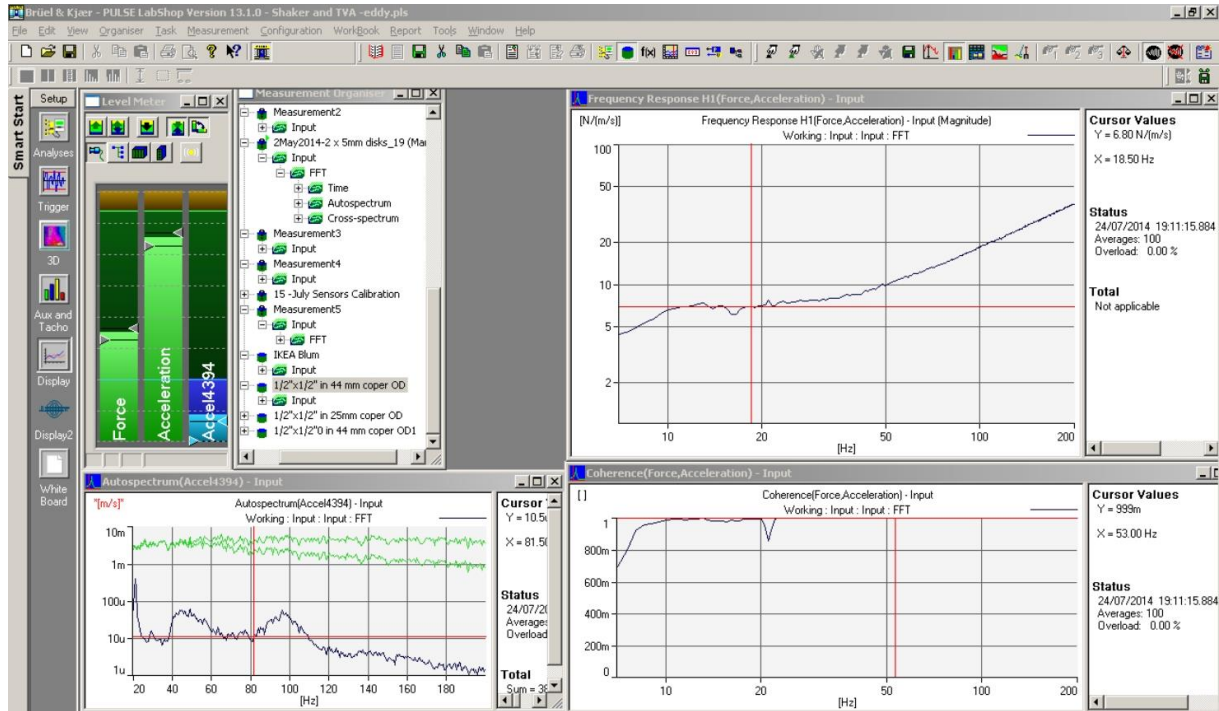
Figure 3 – B&K Pulse FFT analyser screen showing FRF H1- Impedance Magnitude on the top right, Coherence between the Force and Acceleration below and the autopower spectra of the individual signals on bottom left of the screen. Third channel connected to a small accelerometer B&K type 4394 was not used in this case.

Looking at the FRF spectrum, it can be seen that the Impedance curve is relatively flat in the low frequency region where the damping effect of the eddy current is dominant and has a rising slope at frequencies where the mass effect is dominant. The measured impedance matches the theoretical model of a mass and damper system, when the excitation force is applied to the mass and the damper is fixed at one end, while the other end is attached to the moving mass:

$$Z = c + j\omega m \tag{4}$$

Where c is the damping [N·s/m] and m [kg] is the total mass of the magnet and the shaker support including the internal armature (the mass of all the moving parts). The stiffness effect is ignored as the resonance of the system is below the frequency range of the measurement as can be seen from the Impedance spectrum and from source (3).

The copper ring was positioned such as that the magnet's top face was in the middle of the copper ring in the axial direction, i.e. equal distance from both ends of the copper ring. This location was found by the FEA analysis to maximise the damping forces (see below).

The measured damping (c) due to eddy current effect was approximately 6.8 N·s/m.

The FEA model was configured with the same parameters as in the test configuration and analysed. The results shown below in Figure 4 indicate that maximum damping is achieved at a location when one of the magnet faces is at an equal distance from the copper pipe ends. The maximum damping force value is 0.061 N for a velocity of 10 mm/s which corresponds to a damping value of 6.1 N·s/m.
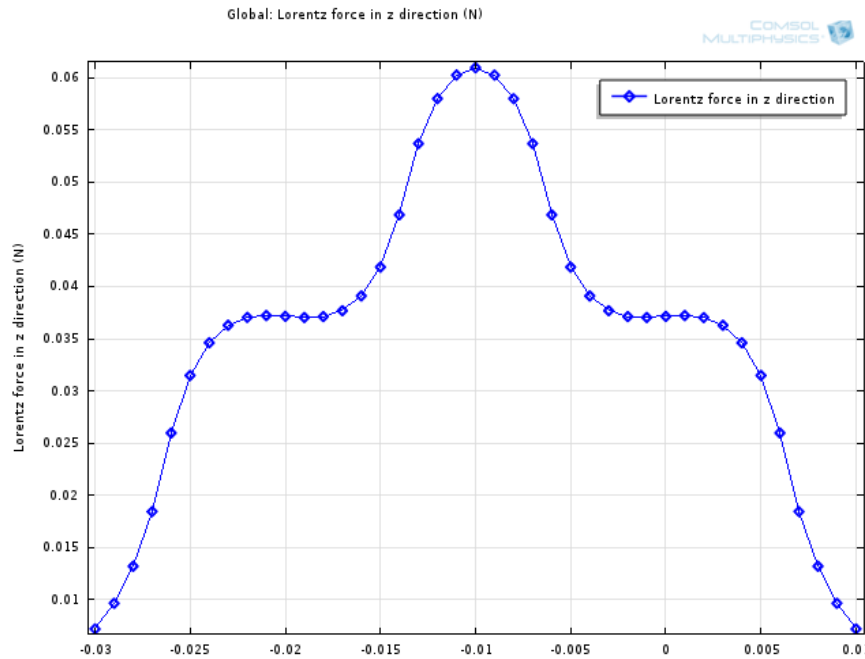
Figure 4 – Lorentz Forces (FL) vs. the Copper Ring relative axial distances (x axis of the figure) relative to

the magnet - for a 10 mm/sec relative velocity. Test Configuration 1

Notice that the curve is symmetrical about the position of maximum force as expected from the physical symmetry of the configuration.

A second test configuration (Config 2) consisted of a magnet with a diameter of 19 mm, 28.2 mm length and the copper ring dimensions were 20mm (ID), 37.7 mm (OD) and 15 mm length. The value of the maximum damping force calculated by the FEA (Figure 5) is 0.12 N for a velocity of 10 mm/s which corresponds to a damping value of 12 N·s/m. This value is within the range of the measured Impedance for Config 2 at low frequencies (7 Hz-15 Hz), which is below the frequency range where the effect of the mass is dominant – see Config 2 curve in Figure 6.
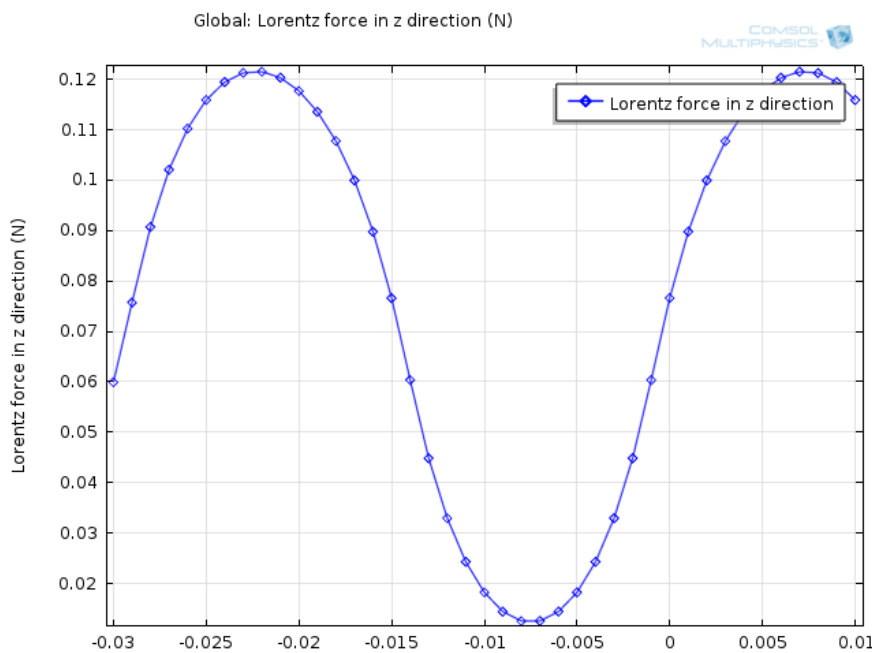

Figure 5 – Lorentz Forces (FL) vs. the Copper Ring relative axial distances (x axis of the figure) relative to

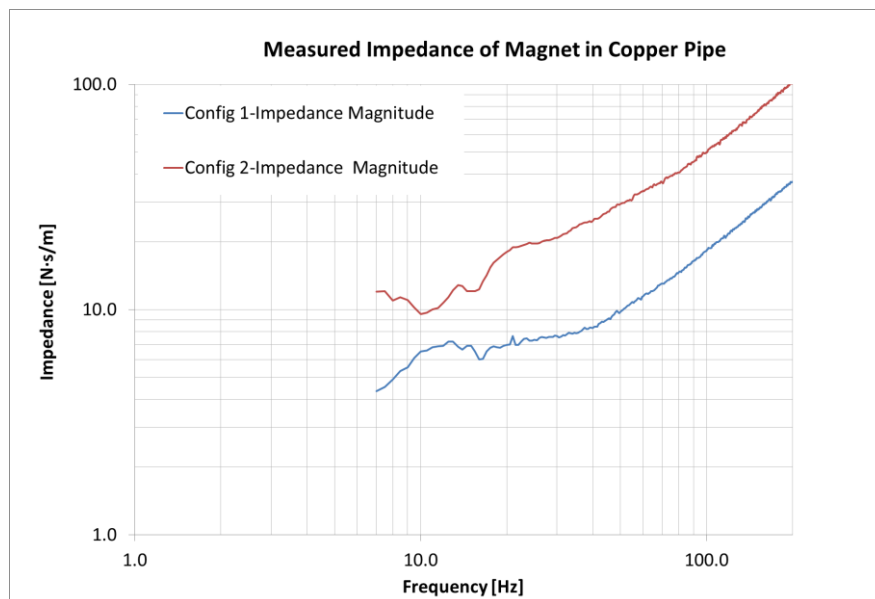the magnet for a 10 mm/sec relative velocity. Test Configuration 2

Figure 6 – Measured Impedance for Magnet in Copper Pipe for two Magnet & Pipe configurations

2.2   The effect of the Relative length of the Magnet and Pipe

When the magnet is shorter than the electrical conducting pipe the maximum damping force is achieved when the centres of the pipe and the magnet are in the same location on the common axis i.e. the faces of the magnet are at the same distance from the near pipe end. However if the magnet is longer than the pipe (ring) the maximum damping occurs at a location where the magnet face that is inside the pipe is at an equal distance from the copper pipe ends. This can be seen by noticing the axial position of the maximum forces value for the two configurations in Figure 4 & 5 above. However between configuration 1 and 2 there are other differences, not only the pipe length, therefore three other configurations were selected such as the only difference between them is the pipe length.

Table 1–Test Configuration for the Investigation of the Length of Pipe effect on Lorentz Forces

Parameter	Configuration 19	Configuration 20	Configuration 21
Magnet strength Br [Tesla]	0.9	0.9	0.9
Magnet Diameter [mm]	12.7	12.7	12.7
Magnet Length [mm]	12.7	12.7	12.7
Pipe Inner Diameter [mm]	13	13	13
Pipe Outer Diameter [mm]	21	21	21
Pipe Length [mm]	**17**	**5**	**26**
Pipe Thickness [mm]	4	4	4
Air Gap [mm]	0.15	0.15	0.15
Velocity [mm/s]	1	1	1

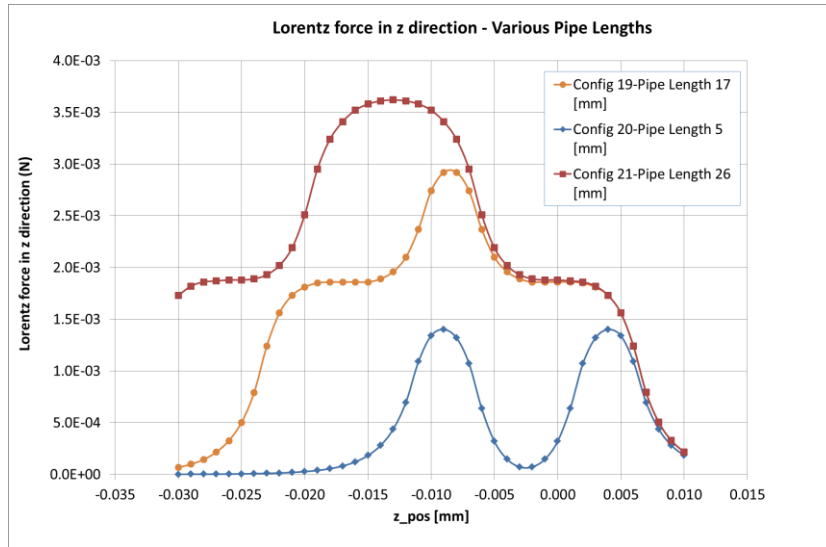The FEA results of the three configurations are plotted in Figure 7.

Figure 7 – FEA calculated Lorentz Forces (FL) vs. the Copper Pipe relative axial distances (graph x axis) relative to the magnet - for 3 pipe lengths.
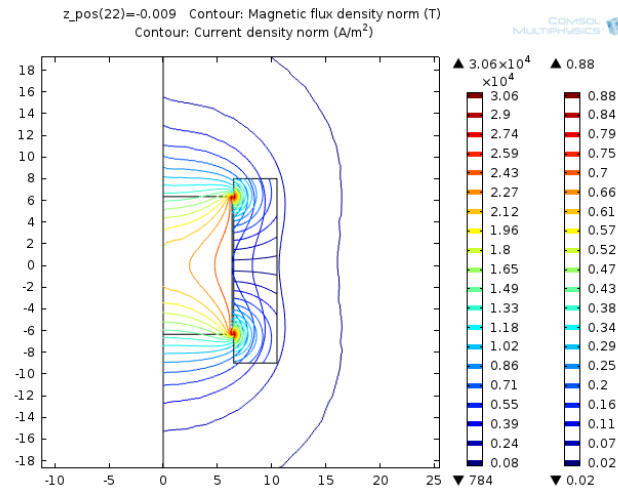

Figure 8 – FEA simulation of the Magnetic Flux Density and the Induced Eddy Currents Density for Configuration 19
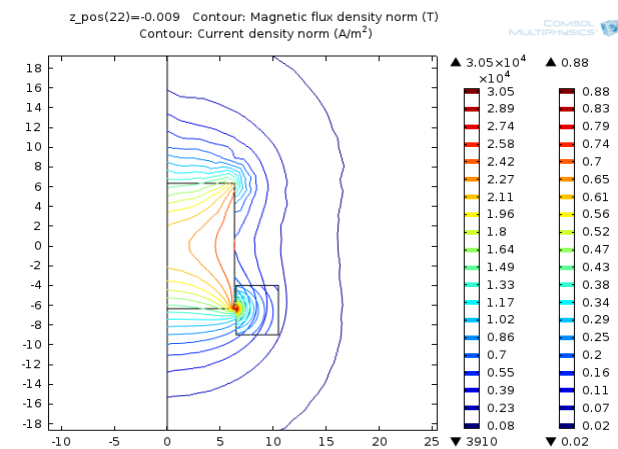

Figure 9 – FEA simulation of the Magnetic Flux Density and the Induced Eddy Currents Density for Configuration 20
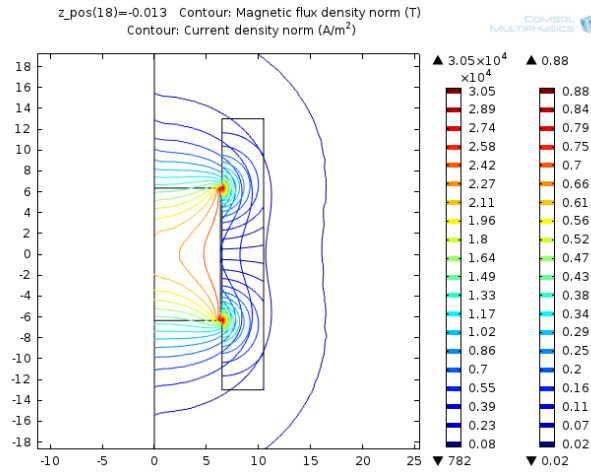
Figure 10 – FEA simulation of the Magnetic Flux Density and the Induced Eddy Currents Density
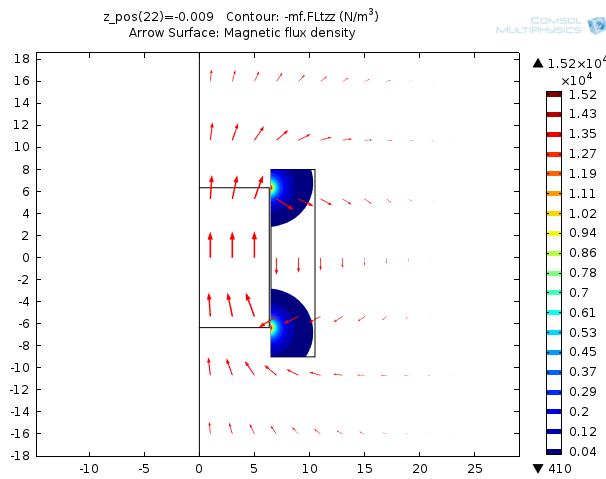for Configuration 21

Figure 11 – FEA simulation of the Magnetic Flux Density Vector and the Lorentz Forces Density
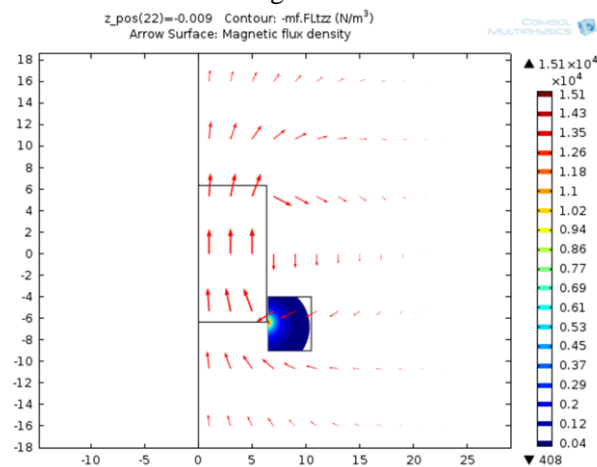for Configuration 19

Figure 12 – FEA simulation of the Magnetic Flux Density Vector and the Lorentz Forces Density
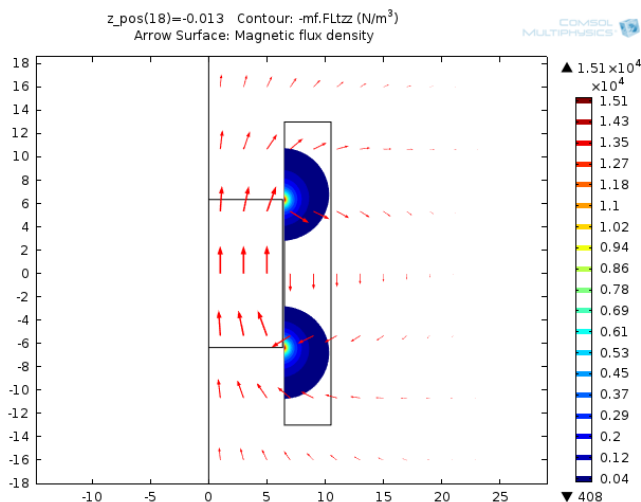for Configuration 20

Figure 13 – FEA simulation of the Magnetic Flux density and the Induced Lorentz Forces Density for Configuration 21

From the images 8 to 13 it can be seen that the maximum damping forces are related to the area (volume) size where there are significant levels of induced eddy currents. Maximum damping forces are obtained when the two ends of the magnet are in the pipe (at equal distances from the end of the pipe - as previously mentioned). Another tentative observation would be that optimal length of the pipe should be such that the distance between the ends of the magnet and the ends of the pipe is about the same as the thickness of the pipe – i.e. a bit shorter than the pipe in configuration 21.

The relationship between pipe length and damping forces is not linear. An exponential based fitting curve of type y= a·(exp(-b·x))+c approximates the data points with a value of R squared equal to 1 (Figure 14). The curve is asymptotically approaching a maximum Lorentz force–i.e. lengthening the pipe length will produce a diminishing increase in the damping forces. The force limit is 0.0049877 N or 4.99 N·s/m for this configuration.
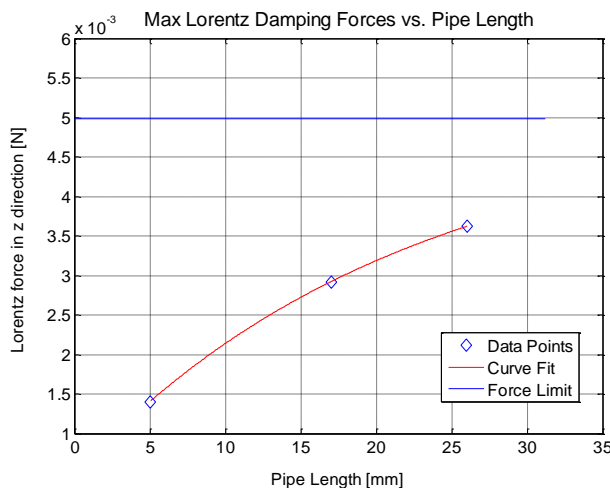

Figure 14 – Lorentz Force on the copper pipe as a function of pipe length.

2.3   Velocity Effect

To investigate the effect of the relative velocity three configurations with the only difference being different velocity values were applied to the copper pipe in the FEA model. The velocities were: 1 mm/sec, 5 mm/sec and 10 mm/sec and the rest of the parameters values are given in Table 2.

Table 2–Test Configuration for the Investigation of the Velocity effect on Lorentz Forces

Parameter	Configuration 17	Configuration 18	Configuration 19
Magnet strength Br [Tesla]	0.9	0.9	0.9
Magnet Diameter [mm]	12.7	12.7	12.7
Magnet Length [mm]	12.7	12.7	12.7
Pipe Inner Diameter [mm]	13	13	13
Pipe Outer Diameter [mm]	21	21	21
Pipe Length [mm]	17	17	17
Pipe Thickness [mm]	4	4	4
Air Gap [mm]	0.15	0.15	0.15
Velocity [mm/s]	**10**	**5**	**1**

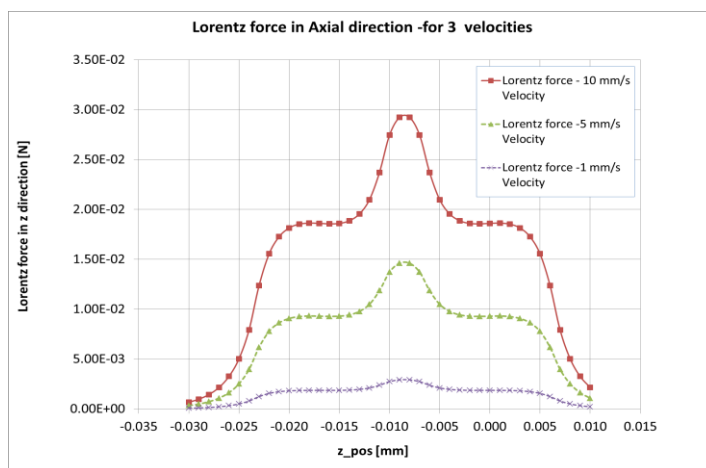The FEA results of the three configurations are plotted in Figure 7 15.

Figure 15 – Lorentz Force on the copper pipe as a function of relative position to the static magnet, for three relative velocities.

As expected the FEA results confirm that forces are proportional to the velocities - Figure 16:
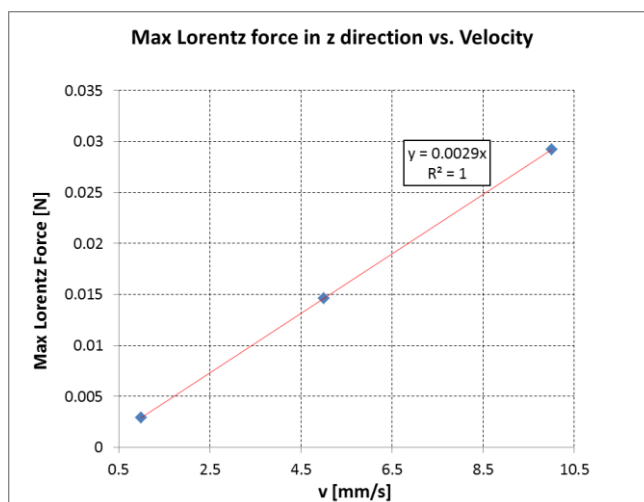

Figure 16 – Lorentz Force on the copper pipe as a function of relative velocities.

When dividing the forces by the respective velocities a constant damping force of 2.92 N·s/m is obtained regardless of the excitation velocity. This behaviour of eddy current damping is the same as viscous damping more commonly employed in commercial dampers and shock absorbers.

2.4 Electrical Conductor Thickness Effect

The effect of the pipe thickness was evaluated by changing the outer diameter of the pipe while the other parameters were the same for the three configurations:

Table 3–Test Configuration for the Investigation of the Thickness Effect on the Lorentz Forces

Parameter	Configuration 13	Configuration 14	Configuration 15
Magnet strength Br [Tesla]	1.1	1.1	1.1
Magnet Diameter [mm]	12.7	12.7	12.7
Magnet Length [mm]	12.7	12.7	12.7
Pipe Inner Diameter [mm]	13	13	13
Pipe Outer Diameter [mm]	**18.85**	**12.5**	**10.5**
Pipe Length [mm]	17	17	17
Pipe Thickness [mm]	**12.35**	**6**	**4**
Air Gap [mm]	0.15	0.15	0.15
Velocity [mm/s]	10	10	10

The FEA results of the three configurations are plotted in Figure 7 17.
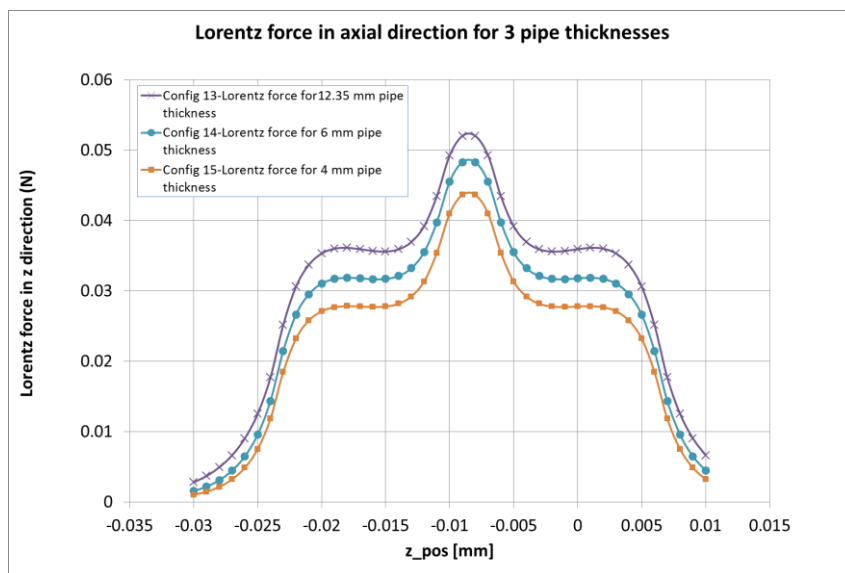

Figure 17 – Lorentz Force on the copper pipe as a function of relative position to the static magnet, for three pipe thickness values.

The relationship between the pipe thickness and damping forces is of an exponential type y= a·(exp(-b·x))+c   as shown in Figure 18.
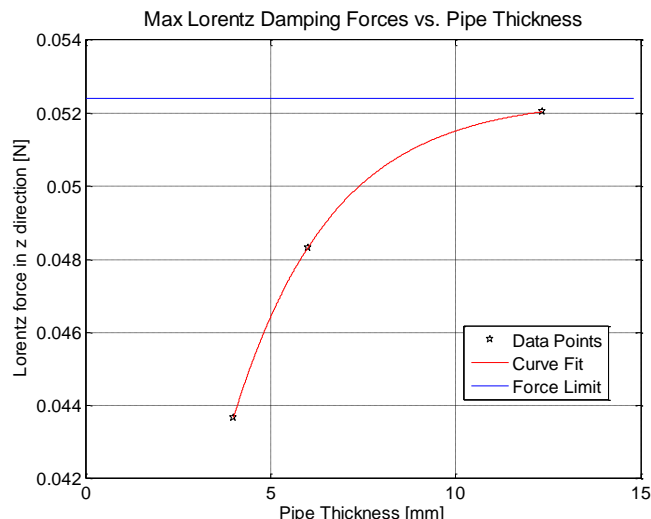
Figure 18 – Lorentz Force on the copper pipe as a function of pipe thickness.

The effect of increasing the thickness of the copper pipe has diminishing benefits on the damping forces, as we have seen before with the pipe length effect. The maximum damping force that can be achieved for this configuration is 0.05241 N or 5.24 N·s/m

2.5   Air Gap Effect

The effect of an air gap is to reduce the strength of the magnetic flux density penetrating the conductor. To achieve various air gaps without changing the pipe thickness both the inner and outer diameter were changed by the same amount. The parameters used in the three configurations are given below.

Table 4–Test Configuration for the Investigation of the Air Gap Effect on the Lorentz Forces

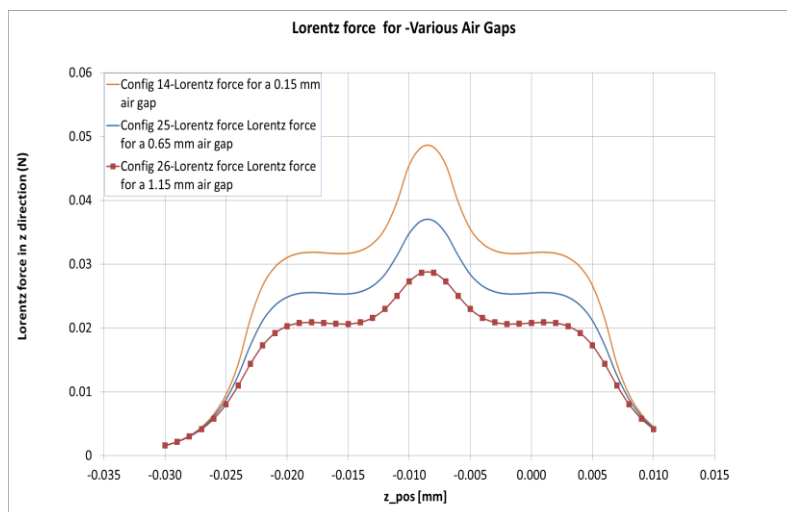| Parameter	Configuration 14	Configuration 25	Configuration 26
Magnet strength Br [Tesla]	1.1	1.1	1.1
Magnet Diameter [mm]	12.7	12.7	12.7
Magnet Length [mm]	12.7	12.7	12.7
Pipe Inner Diameter [mm]	**13**	**14**	**15**
Pipe Outer Diameter [mm]	**25**	**26**	**27**
Pipe Length [mm]	17	17	17
Pipe Thickness [mm]	6	6	6
Air Gap [mm]	**0.15**	**0.65**	**1.15**
Velocity [mm/s]	10	10	10

Figure 19 – Lorentz Force on the copper pipe as a function of relative position to the static magnet, for three air gap values.

As the air gap increases the damping forces are decreasing –fitting the data with an exponential curve gives an R squared value of 0.9995. The curve asymptotically approaches a zero force value as the air gap increases and the maximum force for this configuration when the gap is zero, is predicted to be 0.0521 N or 5.21 N s/m
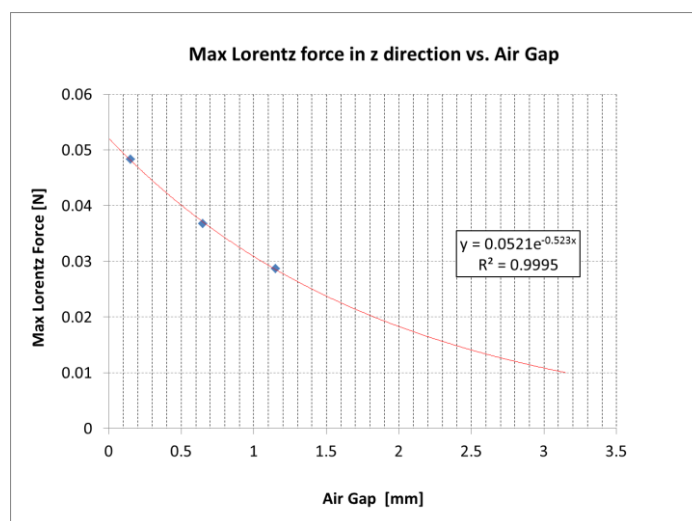

Figure 20 – Lorentz Force on the copper pipe as a function Air Gap values.

3.   CONCLUSIONS

This investigation examined the effects of a number of geometrical and physical parameters on the damping forces experienced by a magnet moving inside an electrical conductive pipe, which are caused by induced eddy currents and their associated magnetic fields. The simple model used in this paper is the basis of eddy currents dampers that may be utilized for attenuating vibrations in vehicles, machinery and structures in general.

Only one parameter was changed each time in order to evaluate the effect of that parameter in isolation. The FEA results matched the test results and the effect of varying each parameter matched the expected

behaviour. Some of the effects of increasing the value of parameters such as the pipe length and pipe thickness on the damping forces is characterised by a "diminishing benefits" behaviour which indicates the potential to optimise the values of the parameters for weight and cost reduction.

In particular there is no benefit to have a magnet longer than the pipe because only one pole is creating the current damping effect.

Further work is required to establish if there are any significant interactions between the parameters, by conducting a factorial or partial factorial experiment design.

REFERENCES

1. Schwartz M. Principles of Electrodynamics: Dover Publications.

2. Bae J-S, Hwang J-H, Park J-S, Kwag D-G. Modeling and experiments on eddy current damping caused by a permanent magnet in a conductive tube. J Mech Sci Technol. 2009;23(11):3024-35.

3. Fox LG. Electrodynamic shaker fundamentals. Sound & Vibration. 1997;31(4):14-23.